



Structural determinants for phosphatidylinositol recognition by Sfh3 and substrate-induced dimer–monomer transition during lipid transfer cycles



Huiseon Yang^a, Junsen Tong^a, Thomas A. Leonard^b, Young Jun Im^{a,*}

^a College of Pharmacy, Chonnam National University, Gwangju 500-757, South Korea

^b Department of Structural and Computational Biology, Max F. Perutz Laboratories, Vienna, Austria

ARTICLE INFO

Article history:

Received 14 February 2013

Revised 13 March 2013

Accepted 5 April 2013

Available online 18 April 2013

Edited by Christian Griesinger

Keywords:

Crystal structure
Lipid transfer protein
Phosphatidylinositol
Sfh3
Sec14

ABSTRACT

Sec14 family homologs are the major yeast phosphatidylinositol/phosphatidylcholine transfer proteins regulating lipid metabolism and vesicle trafficking. The structure of *Saccharomyces cerevisiae* Sfh3 displays a conserved Sec14 scaffold and reveals determinants for the specific recognition of phosphatidylinositol ligand. Apo-Sfh3 forms a dimer through the hydrophobic interaction of gating helices. Binding of phosphatidylinositol leads to dissociation of the dimer into monomers in a reversible manner. This study suggests that the substrate induced dimer–monomer transformation is an essential part of lipid transfer cycles by Sfh3.

Structured summary of protein interactions:

Sfh3 and **Sfh3** bind by X-ray crystallography (View interaction)

Sfh3 and **Sfh3** bind by molecular sieving (View interaction)

© 2013 Federation of European Biochemical Societies. Published by Elsevier B.V. All rights reserved.

1. Introduction

The biogenesis of organelle membranes requires the coordinated transport of proteins and specific lipids from sites of synthesis to sites where they are required. Lipids are moved between cellular compartments by vesicular transport and non-vesicular pathways involving lipid transfer proteins (LTPs). Phosphoinositides (PIs), phosphorylated derivatives of phosphatidylinositol (PtdIns), are important components of membrane-associated signaling systems in eukaryotes where they serve as second messengers and signal integrators [1]. The major phosphoinositide species are concentrated at distinct sites in intracellular membrane trafficking pathways and serve as organelle markers [2]. PtdIns is synthesized in the ER and is subsequently transported to the plasma membrane where it is converted to PIs by phosphatidylinositol kinases [3].

Sec14 of *Saccharomyces cerevisiae* was originally identified as a phosphatidylinositol transfer protein (PITP) that catalyzes the in vitro transport of PtdIns and phosphatidylcholine (PtdCho) between artificial and biological membranes [4]. The protein appears to be multifunctional, with cellular functions ranging from intermembrane phospholipid transport to substrate presentation to

lipid-modifying enzymes. In addition, Sec14 plays an essential role in protein transport from the trans-Golgi complex to the cell periphery [5]. The yeast genome encodes five genes named SFH1–5 (SEC 14 homologues) whose products exhibit significant sequence homology to Sec14 [6]. Sfh1 displays the highest sequence identity (64%) to Sec14. Sfh2–5 represent novel PITPs that exhibit PtdIns – but not PtdCho-transfer activity in vitro [7]. Over-expression of Sfh2, Sfh4, and Sfh5 leads to suppression of *sec14*-related growth and secretion defects. Deletion of SFH3 and SFH4 results in sensitivity to several antifungal drugs [8]. Deletion of SFH3 has a pronounced effect on the sterol composition of plasma membrane, and SFH4 deletion results in alteration of the phospholipid patterns of plasma membrane in yeast [8]. Structural studies of Sfh1 have revealed that it binds the PtdCho and PtdIns headgroups at physically distinct sites [9]. PtdCho-binding and PtdIns-binding are both required for the biological function of Sec14. It was proposed that Sec14 performs heterotypic exchange of PtdCho for PtdIns with regulated conformational transitions [9,10]. These findings led to a model in which Sec14/Sfh1 functions as a nanoreactor for PtdCho-regulated presentation of PtdIns to PtdIns kinases, thereby affecting PI synthesis and regulating specific membrane-trafficking pathways [3,11].

Sfh3 is distantly related to Sec14 and Sfh1, sharing 14% and 18% primary sequence identities (31% and 33% similarity) respectively. Sfh3 localizes to lipid particles and microsomes and catalyzes

* Corresponding author. Fax: +82 62 970 0349.

E-mail address: imyounjung@jnu.ac.kr (Y.J. Im).

PtdIns transfer like Sec14 [12]. However, differences in the residues lining the ligand-binding pocket of Sfh3 compared to Sec14 suggests that it might have a different ligand specificity and a distinct lipid transfer mechanism from Sec14. In addition, the functional properties of Sfh3 are fundamentally different from those of Sec14 and Sfh1 [4,10].

To investigate Sfh3 function and ligand specificities from a structural perspective, we have determined the structures of full-length Sfh3 in the apo form and in complex with phosphatidylinositol. The apo structure reveals a dimeric Sfh3 that is unique to the Sec14 family homologs. Structural and biochemical studies indicate that Sfh3 binds PtdIns, but does not bind PtdCho. PtdIns-binding changes the dimer–monomer equilibrium of Sfh3, which we propose is an essential part of the lipid transfer cycle. From this study, we have derived a model for the phosphatidylinositol transfer cycle.

2. Materials and methods

The expression, purification, crystallization of Sfh3, X-ray data collection, structure determination and refinement are described in Supplementary material. The final refinement statistics are shown in Table 1.

2.1. SEC analysis of Sfh3

DOPC (1,2-dioleoyl-*sn*-glycero-3-phosphocholine), POPS (1-palmitoyl-2-oleoyl-*sn*-glycero-3-phospho-L-serine), were obtained from Avanti Polar Lipids and PtdIns (L- α -phosphatidylinositol from soybean) were obtained from Sigma–Aldrich. For the phospholipid binding assay of Sfh3, each lipid in chloroform was dried under nitrogen stream in glass tubes. Lipid films were resuspended in 50 mM HEPES, pH 7.2, and 120 mM potassium acetate (HK buffer) to a final lipid concentration of 2 mM and sonicated for 3 min. Liposomes were mixed with purified Sfh3 in a 10:1 molar ratio and incubated at room temperature for 24 h. The mixture of Sfh3 and the lipids was analyzed by size exclusion chromatography. The monomeric form of PtdIns loaded Sfh3 was isolated from SEC fractions and used for protein crystallization and lipid transfer assays.

For the SEC analysis of Sfh3–PtdIns samples incubated with liposomes, DOPC and PtdIns in chloroform were mixed at a desired

molar ratio, incubated at 37 °C for 5 min and the solvent evaporated under nitrogen. Dried lipids were resuspended in 1 ml of HK buffer by vortexing. The hydrated lipid mixture was frozen and thawed five times using a water bath and cooled ethanol at –70 °C. The lipid mixture was extruded 10 times through a 0.1 μ m polycarbonate filter. The final lipid concentration of liposomes was 2 mM. The liposomes and PtdIns–Sfh3 were mixed at a desired molar ratio. After incubation at room temperature, samples were centrifuged at 14000 g for 10 min and the supernatants were analyzed by SEC.

3. Results

3.1. Overall structure of Sfh3

The structure of apo Sfh3 from *S. cerevisiae* was determined at 2.0 Å resolution by single anomalous dispersion (SAD) using selenomethionine-labeled Sfh3 (Table 1). The structure consists of 11 α helices and 9 β -strands (Fig. 1A). The structure of Sfh3 consists of two domains held together by an N-terminal extended loop (residues 16–41) and a 34 Å-long C-terminal α helix (α 10) (Fig. 1B). The N-terminal domain consists of five α helices (α 1, α 2, α 3, α 4 and α 11) and two short β strands. The C-terminal domain consists of helices α 5– α 9 and seven β -strands (β 1, β 4– β 8, and β 9) and it contains a large hydrophobic pocket with a surface area of 1500 Å². The core of the C-terminal domain consists of a central five-stranded β sheet (β 4– β 8) sandwiched between three α helices and the C-terminal loop regions. The five β -strands constitute the hydrophobic pocket floor. The α 6 and α 7 helices form one side of the hydrophobic cavity, while α 8 and α 9 form the other side. The seven residues in the β 7– α 7 loop were disordered and not visible in the electron density maps. The interface between the N-terminal and C-terminal domains creates a cavity composed mainly of hydrophilic residues from α 2– α 4 of the N-terminal domain and α 6– α 7 and the α 7– β 7 loop of the C-terminal domain. The hydrophilic cavity has a volume of 600 Å³ and contains 25 ordered water molecules. The α 8 and α 9 helices, known as gating helices of the hydrophobic pocket, are open in the Sfh3 structure (Fig. 1C). The helix α 8 is involved in dimerization by making hydrophobic interactions with helix α 7 of the other protomer.

Table 1
Statistics of data collection and crystallographic refinement.

Crystal	apo Sfh3 Se-Met	apo Sfh3 Native form	Sfh3–PtdIns complex
Construct	Residues 15–345 V100M	Residues 2–350	Residues 15–345
Wavelength (Å)	0.97941 (peak)	0.97949	0.97949
X-ray source	7A, PLS	5C, PLS	5C, PLS
Space group	$P2_1$	$P2_12_12_1$	$P2_1$
Unit cell	$a = 52.7 \text{ \AA}$, $b = 143.6 \text{ \AA}$, $c = 55.8 \text{ \AA}$ $\beta = 111.0$	$a = 53.0 \text{ \AA}$, $b = 113.3 \text{ \AA}$, $c = 144.1 \text{ \AA}$	$a = 52.9 \text{ \AA}$, $b = 144.1 \text{ \AA}$, $c = 55.7 \text{ \AA}$ $\beta = 111.3$
Resolution (Å) (last shell)	1.9 (2.34–2.30)	2.0 (2.03–2.00)	1.55 (1.58–1.55)
No. of unique reflections	32983	59649	111015
Redundancy	3.3 (3.0)	5.1 (5.1)	2.8 (2.7)
$I/\sigma(I)$ (last shell)	23.2 (3.5)	30.2 (4.1)	32.4 (4.3)
R_{sym} (%)	6.7 (30.8)	7.8 (41.2)	4.6 (35.0)
Data completeness (%)	99.4 (98.7)	99.5 (99.1)	99.1 (98.8)
Phasing	Se-SAD	MR	MR
Overall FOM (50–2.3 Å)	0.44 (SOLVE) 0.65 (RESOLVE)		
Refinement			
$R_{\text{work}}/R_{\text{free}}$	21.3/23.5 (24.5/29.3)	23.6/26.1 (26.1/30.7)	22.1/23.9 (24.8/27.1)
R.m.s. bond length (Å)	0.005	0.006	0.005
R.m.s. bond angle (°)	1.2	1.2	1.3
Average B value (Å ²)	19.6	33.4	21.8
Number of atoms	5431 (protein 5274, water 157)	5583 (protein 5313, water 270)	5736 (protein 5358, water 319, PtdIns 59)

The values in parentheses relate to highest resolution shells.

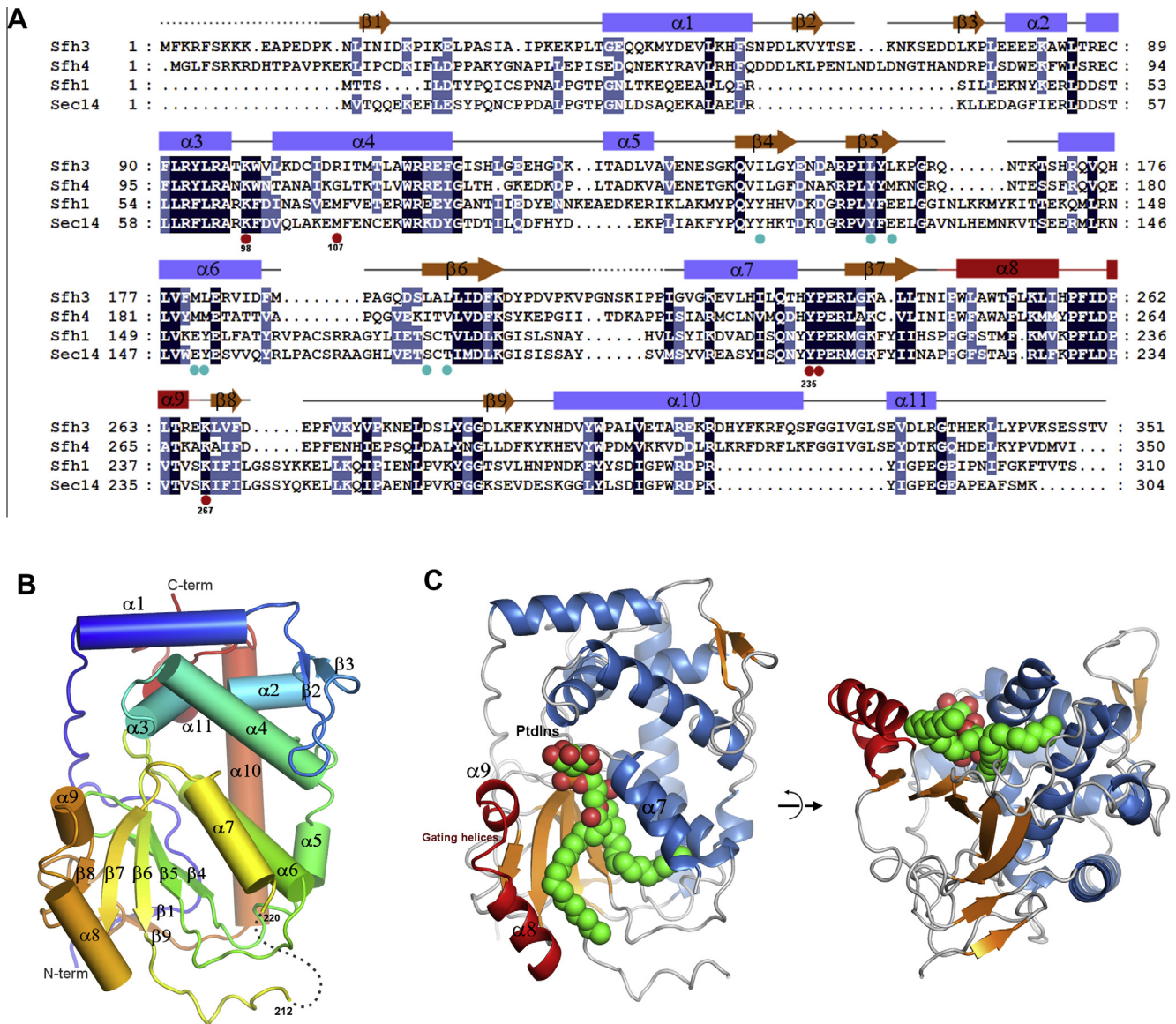


Fig. 1. Overall structure of Sfh3. (A) Sequence alignment of yeast Sec14 family homologs. The conserved hydrophilic residues recognizing the inositol head group of PtdIns are indicated with red circles. The variable residues involved in PtdCho binding in Sec14 and Sfh1 homologs are indicated in green dots. The secondary structure elements of gating helices $\alpha 8$ and $\alpha 9$ were colored red. (B) Cartoon representation of apo Sfh3 structure (C) Ribbon representation of PtdIns-bound Sfh3 monomer. Secondary structure elements are colored to match those of (A).

3.2. Sfh3 forms a dimer in a ligand free state

Size exclusion chromatography (SEC) analysis demonstrated that the recombinant Sfh3 is a homogeneous dimer without a detectable monomeric species, suggesting that dimeric Sfh3 is a biologically relevant form (Fig. 2A). Dimeric Sfh3 was also reported in a previous purification and crystallization study [13]. Sfh3 crystallized as a dimer in the asymmetric unit with molecular dimensions of $94 \times 60 \times 55 \text{ \AA}$. The protomers in the dimer are related by a non-crystallographic twofold axis (Fig. 2B). The dimer interface is formed by association of two hydrophobic binding pockets from each protomers. The gating helices $\alpha 8$ and $\alpha 9$ in an open conformation compose the center of the two-fold axis in the dimer. Dimerization buries total 2048 \AA^2 of surface area in two protomers. The dimer is stabilized by two hydrogen bonds in the $\alpha 8$ – $\alpha 9$ loop and hydrophobic interactions between the $\alpha 7$ and $\alpha 8$ helices (Fig. 2C). The eight hydrophobic residues in helix $\alpha 8$ make hydrophobic interaction with helix $\alpha 7$ of the other protomer. Helix $\alpha 8$ from the other protomer occu-

pies a position close to where $\alpha 8$ is expected to be positioned in the closed conformation of Sfh3, resulting in formation of empty cavities in the ligand binding pockets of each protomer in the dimer. However, the ligand binding pockets are partially accessible for ligand binding from the solvent in the dimeric state. Dissociation of the dimer into monomers seems to be essential for the binding of PtdIns ligand. To prove this hypothesis, oligomeric states of Sfh3 proteins incubated with various phospholipids including PtdIns, PtdCho and PtdSer were analyzed by SEC. The apo Sfh3 is a dimer. We did not observe a monomeric species during the purification steps that are free of PtdIns. Incubation of Sfh3 with PtdIns at a 1:10 molar ratio dissociated the dimer into an exclusively monomeric form indicating that Sfh3 is loaded with PtdIns ligand (Fig. 2A). Binding of the ligand to Sfh3 would induce a closure of the gating helices which inhibits dimerization by deforming the structure of dimer interface. In contrast, incubation with PtdCho or PtdSer had no effect on the oligomeric states of Sfh3 implying that Sfh3 selectively binds to PtdIns.

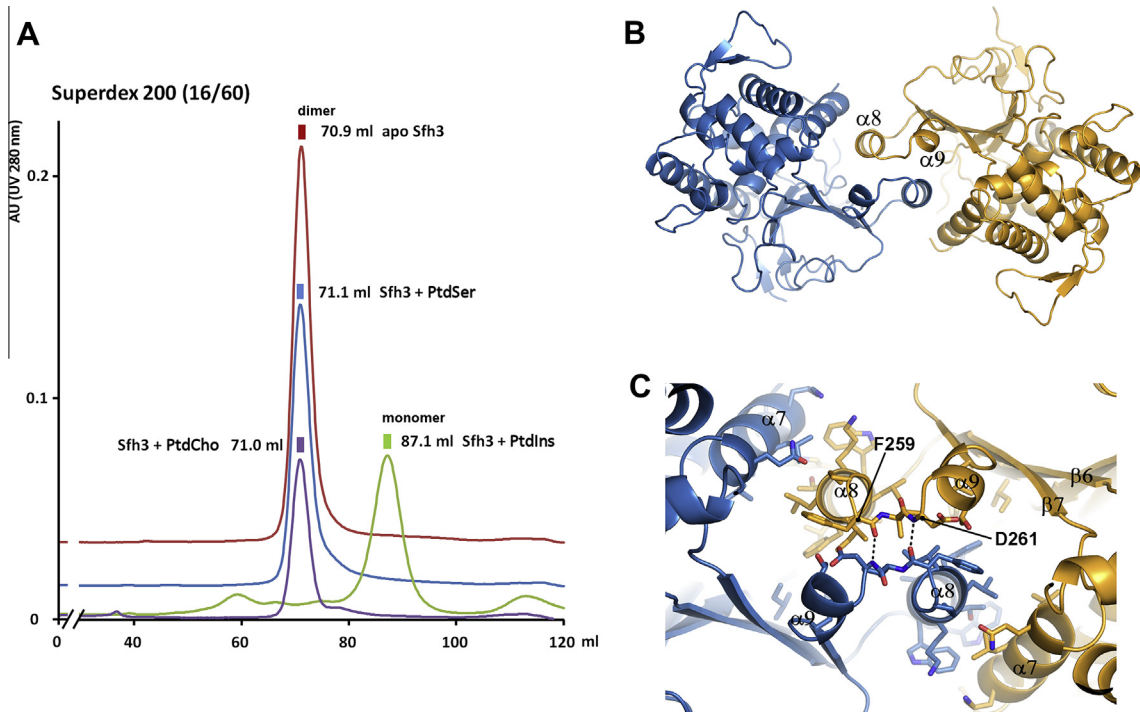


Fig. 2. Dimeric structure of apo Sfh3. (A) SEC profiles of Sfh3 samples incubated with various phospholipids. (B) Overall structure of dimeric Sfh3. (C) Dimer interface of Sfh3.

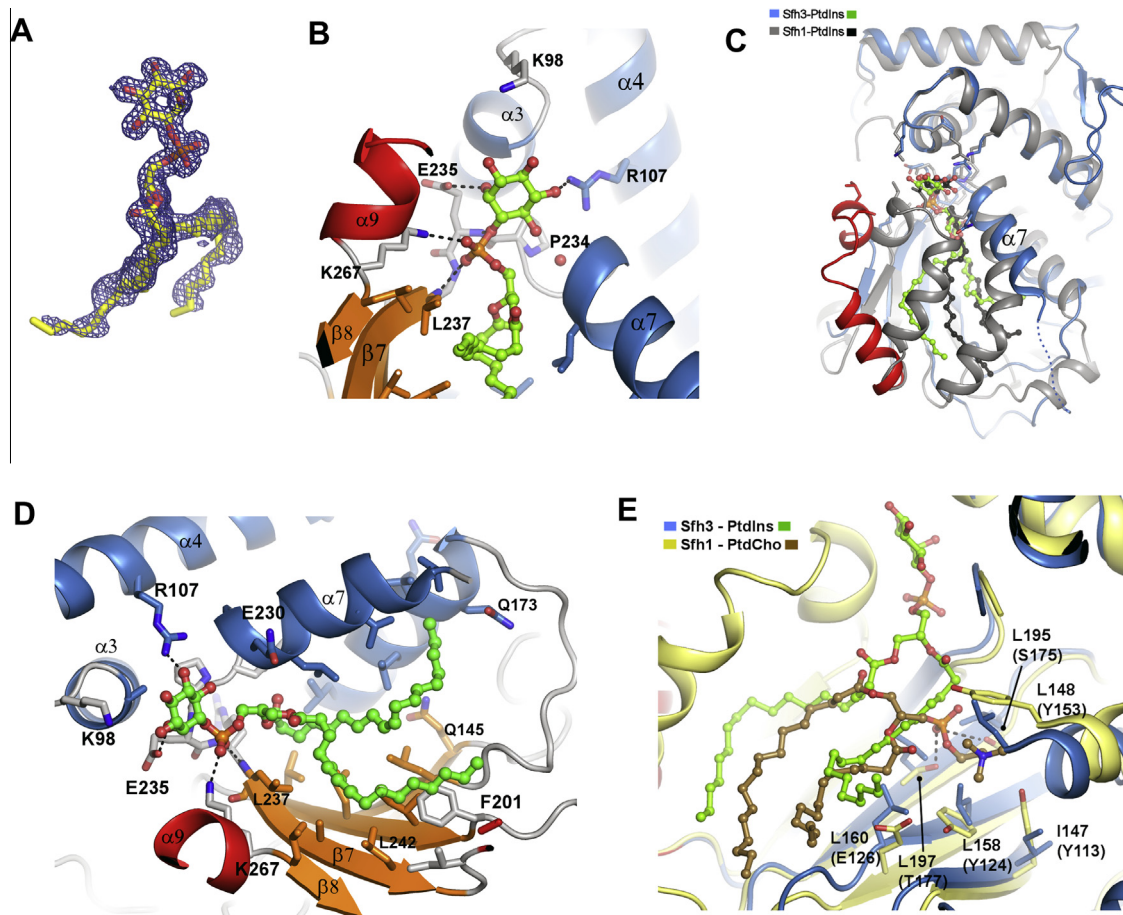


Fig. 3. PtdIns binding site of Sfh3. (A) 2Fo-Fc electron density map on bound PtdIns in Sfh3 contoured at 0.8 σ . (B) Binding site of PtdIns head group. (C) Overview of PtdIns binding in the hydrophobic pocket of Sfh3. (D) Structural comparison of PtdIns-bound Sfh1 and Sfh3. (E) Superposition of the ligand binding sites of Sfh1-PtdCho and Sfh3-PtdIns complexes. The labels in parenthesis correspond to Sfh1.

3.3. Structure of Sfh3–PtdIns reveals substrate specificity

To elucidate the structural determinants of PtdIns binding, Sfh3 was loaded with soybean PtdIns, crystallized, and the structure determined to 1.55 Å resolution by molecular replacement using apo-Sfh3 (Table 1). The PtdIns molecule is well ordered in the structure with strong electron density for the head group of the ligand and traceable density for the two acyl chains (Fig. 3A). The PtdIns was modeled as the 18:0/18:1 molecular species. The PtdIns is incorporated into the Sfh3 binding cavity in an orientation such that the inositol headgroup is coordinated near the protein surface and the acyl chains in the hydrophobic pocket. The phospho-inositol moiety of bound PtdIns forms extensive contacts with residues from $\alpha 2$, $\alpha 3$, and $\alpha 9$ helices, and the $\alpha 7$ – $\beta 7$ and $\alpha 8$ – $\beta 9$ loops. The Sfh3–PtdIns interactions involve seven hydrogen bonds with the PtdIns headgroup (Fig. 3B). The headgroup phosphate is coordinated by the main-chain amide nitrogens of Glu235, Arg236, Leu237 and by the side chain of Lys241. The 2-hydroxyl group of the inositol ring makes a hydrogen bond with the side chain of Glu235, and the 4-hydroxyl group interacts with Arg107 ($\alpha 4$). In addition, the 6-hydroxyl group makes a water-mediated contact to the N-terminal end of helix $\alpha 7$. The two acyl chains of PtdIns make extensive hydrophobic interaction with hydrophobic residues on the bottom and the wall of the binding pocket in a non-specific manner, as suggested by weak and ill-defined electron density maps in these regions (Fig. 3C).

Structural comparison of Sfh3 with Sec14 and Sfh1 reveals the determinants for ligand specificities. The sequences and the

geometries of the residues involved in the recognition of the phosphoinositol head group are well conserved in Sec14 superfamily proteins indicating that PtdIns is a common ligand (Fig. 3D). In addition, the sequence and shape of the gating helices are similar in Sfh1 and Sfh3, though Sfh3 has an open conformation of gating helices. In Sfh3, the N-terminal upstream region of helix $\alpha 7$ is disordered while this region forms an α -helix in Sfh1. The major functional difference of Sfh3 from Sfh1 and Sec14 is the lack of PtdCho binding activity. Sfh1 binds both PtdIns and PtdCho in overlapping binding sites for two acyl chains but the head groups of each ligands are recognized by distinct sites in the hydrophobic pocket. The head group of PtdCho is recognized by a cluster of hydrophilic residues in the floor of the hydrophobic pocket formed by the β -sheet of the C-terminal domain in Sfh1. The Structure of Sfh3 explains why it is incapable of binding PtdCho. The six hydrophilic residues that recognize the head group of PtdCho in Sfh1 are all hydrophobic residues in Sfh3 (Fig. 3E). The hydrophobic character in the pocket floor excludes binding of any polar groups such as the choline moiety of PtdCho.

3.4. Structural comparison of apo Sfh3 and Sfh3–PtdIns complex

Superposition of apo-Sfh3 and PtdIns-loaded Sfh3 indicates almost identical conformations of monomers (C_{α} rmsd = 0.28 Å). The structural differences between the apo-form and the ligand complex are the presence of PtdIns in the binding site and the slight conformational adjustments of side chains of the ligand binding residues. Unexpectedly, even though the monomeric

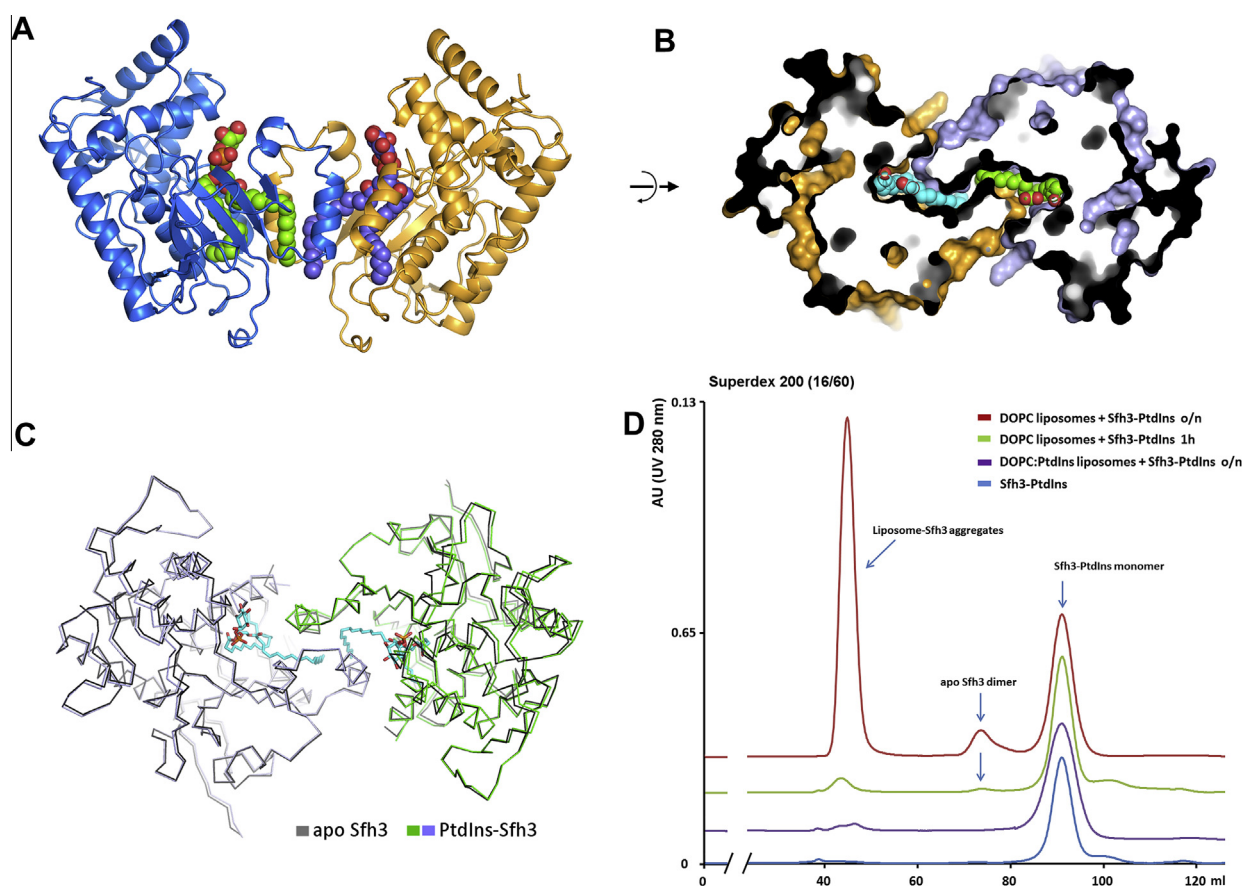


Fig. 4. Oligomeric states of Sfh3. (A) Dimeric structure of PtdIns bound Sfh3. (B) Surface representation of PtdIns bound Sfh3 dimer. (C) Structural comparison of apo dimer and PtdIns bound dimers. (D) Size exclusion chromatography profiles of PtdIns–Sfh3 incubated with various liposomes. The 1 mg of PtdIns-loaded Sfh3 was mixed with the 2 mM of liposomes at a 1:50 molar ratio resulting in 0.03 mM of a final protein concentration. For the sample corresponding to redline, 3 mg of PtdIns–Sfh3 was mixed with liposomes at a 1:50 molar ratio and incubated for 14 h prior to SEC analysis.

PtdIns-bound Sfh3 was used for crystallization, the crystal structure of Sfh3–PtdIns complex showed an almost identical dimer observed in the apo Sfh3 with C_{α} rmsd of 0.67 Å for dimers (Fig. 4A–C). SEC analysis of the crystallized drop solution containing PtdIns–Sfh3 crystals indicates a mixture of monomeric and dimeric species, while the drop solutions lacking crystals have only monomeric species (data not shown). It is likely that the dimeric configuration of PtdIns–Sfh3 was induced by lattice formation during the crystallization process. The ligand-bound monomer in a closed form would undergo a conformational change of gating helices to the open form for dimerization. Despite the dimeric structure of PtdIns-bound Sfh3 could be a crystallographic artifact, the structure of each protomer in the dimer with the open conformation might represent the structure of a transient membrane bound form during lipid transfer.

3.5. Dimer–monomer transition of Sfh3 is regulated by substrate binding

To examine whether the PtdIns-induced change of oligomeric states of Sfh3 is reversible, we analyzed the oligomeric state of Sfh3 after incubating the PtdIns-loaded Sfh3 with several liposomes of different lipid compositions (Fig. 4D). We hypothesized that the transfer of bound PtdIns to liposomes would generate unliganded Sfh3 that would spontaneously re-dimerize. The PtdIns-loaded Sfh3 used in the experiment was exclusively monomeric (blue line). When PtdIns–Sfh3 was mixed with pure DOPC liposomes at a 1:50 molar ratio and incubated for an hour, a very small fraction of dimeric Sfh3 was formed (green line). We assumed that the equilibrium is leaned toward PtdIns extraction rather than PtdIns transfer to DOPC liposomes due to the high affinity of Sfh3 to PtdIns. In order to observe the dimer peak more clearly, we increased the amount of protein and liposomes by using triple sample volumes and incubated for 14 h (red line). In this setup, the formation of Sfh3 dimer was clearly visible. A large fraction of Sfh3 was observed at the end of the void volume in SEC, indicating liposome bound Sfh3. Still, the significant fraction of Sfh3 remained as a monomer probably due to the non-ideal condition of

liposomes for lipid transfer compared to the physiological membranes containing various lipids and other protein components. The oligomeric state other than dimer or monomer was not observed suggesting that the formation of Sfh3 dimer is a specific outcome of ligand transfer. We exclude the possibility of artificial dimer formation simply by a high protein concentration in this experiment, because PtdIns–Sfh3 at 15 mg/ml stays as homogeneous monomers when liposomes are absent. In contrast, when DOPC liposomes were doped with 10% PtdIns, no dimeric Sfh3 appeared due to the suppression of the ligand transfer by the presence of PtdIns in the acceptor membrane. This experiment suggests that the dimer–monomer transition is regulated by PtdIns binding in a reversible manner.

4. Discussion

Sec14 of *S. cerevisiae* catalyzes transport of PtdIns and PtdCho between lipid membranes. Sec14 family homologs are proposed to have two major conformations that are the ‘open’ form and the ‘closed’ form. The ‘closed’ form with a bound lipid represents the protein structure in solution [3,14]. The primary difference between the ‘open’ and ‘closed’ conformers is the repositioning of a helical gate by up to 18 Å so that it closes the lipid binding pocket. The open form approximates the conformer(s) involved in lipid exchange on membrane surfaces since it exposes the hydrophobic pocket suitable for membrane binding and lipid extraction. The open form of unliganded PTP is unlikely present in solution since it exposes the extensive hydrophobic surface to the solvent. Consistently, the structure of the open form of a PTP has only been observed in complex with detergents bound to the hydrophobic binding pocket of Sec14 [15]. The ligand binding pockets of Sec14 proteins including Sfh1 seems to be always occupied by PtdIns or PtdCho during the heterotypic lipid transfer cycles except for the transient membrane bound state for lipid exchange [9]. For Sec14 and Sfh1, the transport of PtdIns from the donor membrane to the acceptor membranes requires delivery of PtdCho back to the donor membrane to complete a heterotypic lipid transfer cycle (Fig. 5). All PTPs characterized to date are monomers as a

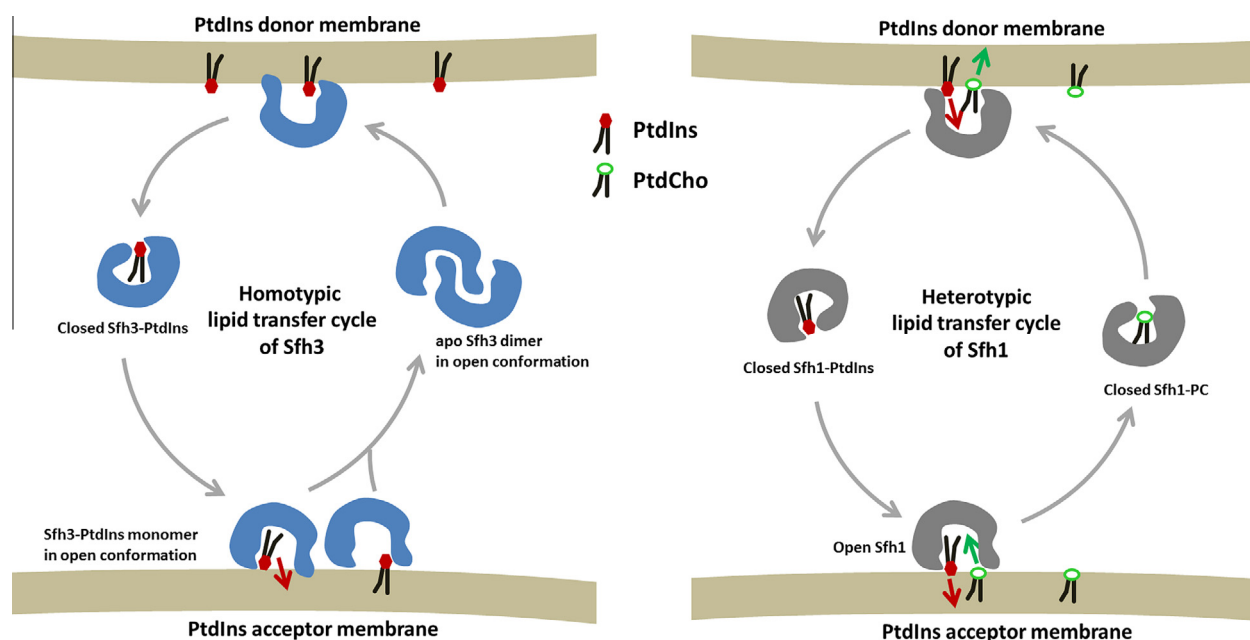


Fig. 5. Schematic models of lipid transfer cycles by Sfh3 and Sfh1. The lipid transfer cycle of Sfh3 was proposed based on this study. The heterotypic lipid transfer model of Sfh1 was based on the previous studies [3,9]. The other protein components such lipid modifying enzymes on the membranes were omitted in these models.

physiologically active form [11]. In contrast, apo Sfh3 has an open conformation of the gating helices which is distinct from Sec14 homologs. Dimerization of Sfh3 seems to allow this exception by partially shielding the hydrophobic ligand binding pocket from the solvent. In addition, dimerization of unliganded Sfh1 explains the homotypic ligand transfer model that does not require binding of the secondary phospholipid for reverse transport. This is consistent with the lack of a PtdCho binding site in Sfh3. Based on these results we propose a model for homotypic lipid transfer cycles of Sfh3 (Fig. 5). Sfh3 performs a unidirectional transport of PtdIns to acceptor membranes. Instead of counter-transporting PtdCho to complete the cycle, Sfh3 recycles as unliganded dimers to the donor membranes.

In summary, this study reveals that the ligand binding properties and molecular mechanisms of Sfh3 are different from Sec14/Sfh1. The structure of Sfh3 at 1.55 Å provides accurate details of the PtdIns recognition in the ligand binding pocket. The results described here provide clear validation for the homotypic lipid transfer mode of Sfh3. How the distinct ligand specificity of Sfh3 translates into its biological function, however, still remains to be elucidated.

5. PDB accession number

Coordinates and structure factors for apo Sfh3 and Sfh3–PtdIns complex have been deposited at the Protein Data Bank with accession codes 4J7P and 4J7Q, respectively.

Acknowledgements

This project was supported by Basic Science Research Program through the National Research Foundation of Korea (NRF) funded by the Ministry of Education, Science and Technology (grant nos. NRF-2010-0013448 and NRF-2011-0025110).

Appendix A. Supplementary data

Supplementary data associated with this article can be found, in the online version, at <http://dx.doi.org/10.1016/j.febslet.2013.04.009>.

References

- [1] Strahl, T. and Thorner, J. (2007) Synthesis and function of membrane phosphoinositides in budding yeast, *Saccharomyces cerevisiae*. *Biochim. Biophys. Acta* 1771, 353–404.
- [2] Roth, M.G. (2004) Phosphoinositides in constitutive membrane traffic. *Physiol. Rev.* 84, 699–730.
- [3] Bankaitis, V.A., Ile, K.E., Nile, A.H., Ren, J., Ghosh, R. and Schaaf, G. (2012) Thoughts on Sec14-like nanoreactors and phosphoinositide signaling. *Adv. Biol. Regul.* 52, 115–121.
- [4] Szolderits, G., Hermetter, A., Paltauf, F. and Daum, G. (1989) Membrane properties modulate the activity of a phosphatidylinositol transfer protein from the yeast, *Saccharomyces cerevisiae*. *Biochim. Biophys. Acta* 986, 301–309.
- [5] Bankaitis, V.A., Aitken, J.R., Cleves, A.E. and Dowhan, W. (1990) An essential role for a phospholipid transfer protein in yeast golgi function. *Nature* 347, 561–562.
- [6] Griac, P. (2007) Sec14 related proteins in yeast. *Biochim. Biophys. Acta* 1771, 737–745.
- [7] Li, X., Routt, S.M., Xie, Z., Cui, X., Fang, M., Kearns, M.A., Bard, M., Kirsch, D.R. and Bankaitis, V.A. (2000) Identification of a novel family of nonclassical yeast phosphatidylinositol transfer proteins whose function modulates phospholipase D activity and Sec14p-independent cell growth. *Mol. Biol. Cell* 11, 1989–2005.
- [8] van den Hazel, H.B., Pichler, H., do Valle Matta, M.A., Leitner, E., Goffeau, A. and Daum, G. (1999) PDR16 and PDR17, two homologous genes of *Saccharomyces cerevisiae*, affect lipid biosynthesis and resistance to multiple drugs. *J. Biol. Chem.* 274, 1934–1941.
- [9] Schaaf, G., Ortlund, E.A., Tyeryar, K.R., Mousley, C.J., Ile, K.E., Garrett, T.A., Ren, J., Woolls, M.J., Raetz, C.R., Redinbo, M.R. and Bankaitis, V.A. (2008) Functional anatomy of phospholipid binding and regulation of phosphoinositide homeostasis by proteins of the sec14 superfamily. *Mol. Cell* 29, 191–206.
- [10] Schaaf, G., Dynowski, M., Mousley, C.J., Shah, S.D., Yuan, P., Winklbauer, E.M., de Campos, M.K., Trettin, K., Quinones, M.C., Smirnova, T.I., Yanagisawa, L.L., Ortlund, E.A. and Bankaitis, V.A. (2011) Resurrection of a functional phosphatidylinositol transfer protein from a pseudo-Sec14 scaffold by directed evolution. *Mol. Biol. Cell* 22, 892–905.
- [11] Bankaitis, V.A., Mousley, C.J. and Schaaf, G. (2010) The Sec14 superfamily and mechanisms for crosstalk between lipid metabolism and lipid signaling. *Trends Biochem. Sci.* 35, 150–160.
- [12] Schnabl, M., Oskolkova, O.V., Holic, R., Brezna, B., Pichler, H., Zagorsek, M., Kohlwein, S.D., Paltauf, F., Daum, G. and Griac, P. (2003) Subcellular localization of yeast Sec14 homologues and their involvement in regulation of phospholipid turnover. *FEBS J.* 270, 3133–3145.
- [13] Ren, J., Schaaf, G., Bankaitis, V.A., Ortlund, E.A. and Pathak, M.C. (2011) Crystallization and preliminary X-ray diffraction analysis of Sfh3, a member of the Sec14 protein superfamily. *Acta Crystallogr., Sect. F: Struct. Biol. Cryst. Commun.* 67, 1239–1243.
- [14] Ryan, M.M., Temple, B.R., Phillips, S.E. and Bankaitis, V.A. (2007) Conformational dynamics of the major yeast phosphatidylinositol transfer protein sec14p: insight into the mechanisms of phospholipid exchange and diseases of sec14p-like protein deficiencies. *Mol. Biol. Cell* 18, 1928–1942.
- [15] Sha, B., Phillips, S.E., Bankaitis, V.A. and Luo, M. (1998) Crystal structure of the *Saccharomyces cerevisiae* phosphatidylinositol-transfer protein. *Nature* 391, 506–510.